FFR120 Simulation of complex systems: Project report
A study of crowd disasters with force-based modeling and fluid dynamics analysis

Team Butterfly
Artur Gasparyan, Maria Li López Bautista, Nina Uljanić, Ruiqi Qiu, and Rundong Zhou
M.Sc. in Complex Adaptive Systems, Chalmers University of Technology
(Dated: January 10, 2023)

Abstract: Crowd crushes are a rare phenomena which result in great number of casualties. Large crowds of people have been found to exhibit fluid-like behavior and can therefore be studied using fluid dynamics. By simulating a crowd using the social force model, and analysing the outcome of the results, we identify the crowd size and velocity as key metrics which strongly correlate with casualties in the crowd, when compared to other metrics such as room width. We also define a pseudo-Reynolds number for the crowd and find that casualties occur when this number is around 250 or larger. The findings show that room design plays a key role in the number of causalities which occur during crowd disasters. Future work could be done with larger scale simulations in order to analyse the fluid dynamics in more depth.

I. INTRODUCTION

The dynamics of human crowds is an interesting yet highly complex topic. Large human crowds exhibit fluid-like collective behavior [1]. The interactions between individuals can, under certain conditions, lead to transitions in the state of the system. When a crowd becomes dangerously overcrowded, i.e., it reaches a specific density threshold, a catastrophic incident known as crowd crush may occur [2]. Crowd crushes are rare, but when they do occur, they produce a large number of casualties [3]. Therefore, they are considered to be a type of non-environmental public disaster [4]. Some notable examples of crowd crushes are the Hillsborough Stadium disaster (1989) [5], Hajj pilgrimage stampede (2015) [6], and more recently the Halloween crowd crush in Seoul, South Korea, which happened in October 2022 [7].

Large concentrations of people occur frequently in modern society. It is therefore important to study the properties of crowds to better understand how to prevent crowd crushes and consequently reduce the number of casualties. To study crowd dynamics, one can use computer simulations with the goal of finding the key factors that lead to crowd disaster scenarios [8].

Various simulation techniques have been developed to simulate crowd dynamics. Yang et al. [9] provide a summary of the most notable crowd simulation models, that is, those which are widely used. They established that the existing models can be grouped into three major categories: microscopic models, which are characterized by low-level behavioral details, macroscopic models, which consider the crowds to be an unified and continuous entity, and mesoscopic models, which lie between the other two. Microscopic models are most abundant, and here one can find rule-based models, force-based models, and agent-based models, to name a few. Among these, we have found the ideal candidates for our simulation.

In this project, we study the behavior of a crowd using computer simulations. Taking into account the similarities between a human crowd and classical fluids, we define some coefficients, §II A, that help us determine the state of the crowd. In addition, we analyze its dependence on various parameters, further explained in §II C.

We show that crowd size and velocity are key parameters that impact the number of casualties in the crowd and that the room design plays an important role in affecting casualties. The crowd crush happened under certain conditions which are influenced by many factors. An extreme setting can have serious consequences, while a combination of different rigorous settings can also lead to casualties.

In §II the models and forces used in the simulation are explained, and the implementation is described. The results of the project are reported in §III in addition to a brief discussion of the findings. §IV contains the conclusion of the project and discusses potential future work.

II. METHODOLOGY

To begin with, we simulate the dynamics of a crowd using a force-based model [10, 11] that takes into account the interacting forces between individuals via Newton's second law of motion. As a result, we obtain the evolution of the positions, velocities, and net forces of each individual, as well as the global density of the crowd. We analyze these data by treating the crowd as a fluid [1, 12, 13].

A. Fluid analogy

The dynamics of fluids provide the necessary foundations to understand the flow of fluids, gases, and liquids. Its applications can be found in the study of the motion of air (aerodynamics) or the movement of liquids in streams (hydrodynamics), such as water, lava, and so forth. Thus, it provides the essence for comprehending the behavior of complex systems such as the atmosphere

and oceans [14].

In fluid mechanics, the ratio between inertial and viscous forces acting on a flowing fluid can be measured using the so-called Reynolds number [15]. In general, the definition of this parameter includes the fluid properties of density and viscosity, plus a velocity and a characteristic length or dimension. Furthermore, this dimensionless quantity helps predict fluid patterns in different situations, since at low Reynolds numbers, flows tend to be dominated by laminar behaviors, while at high Reynolds numbers, flows tend to be turbulent [16]. More particularly, laminar flow is the case when the friction is high at the boundaries and the fluid exhibits smooth, parallel, and steady streamlines. Meanwhile, a turbulent flow is represented by irregular streamlines that change over time. Therefore, the different parts of the fluid mix together or create small circular regions that resemble whirlpools [17].

In this project, in comparison with classical fluid mechanics [18], we define our own dimensionless Reynolds number of the crowd,

$$\mathrm{Re}_c = \frac{\rho v_\mathrm{d} L}{\eta}, \tag{1}$$

where ρ and v_d are, respectively, the number of people per unit area [L^{-2}] and the individual desired speed of the crowd [LT^{-1}] (highly related to the stress level of the crowd), L is the length of the room [L], and η is the number of people passing through the exit per unit of time [T^{-1}], which plays the role of fluid viscosity.

The construction of this pseudo-Reynolds [1] number allows us to carry out a qualitative analysis of the state of the crowd. For instance, at low Reynolds numbers, the individuals have a higher exit rate, meaning that the crowd is moving in an ordered manner, which corresponds to the laminar state of a fluid. On the contrary, when the Reynolds number is high, the crowd might be denser and more susceptible to collisions that provoke clustering and chaotic motion, which is analogous to the turbulent state of a fluid.

Furthermore, we can define an alignment coefficient of the crowd,

$$\Psi_c = \frac{1}{N}\left\|\sum_{i=1}^{N}\frac{\mathbf{v}_i}{v_d}\right\|, \tag{2}$$

at each time step to determine the direction of the flow, where N is the number of people, $\mathbf{v_i}$ the velocity of each individual, and v_d is the desired speed of the individual.

The alignment coefficient is an important parameter for detecting if turbulence is occurring in the simulation, i.e., if $\Psi_c \sim 1$, the velocities of individuals are highly aligned, and thus the crowd is in the laminar state. If $\Psi_c \sim 0$, the alignment is low, representing the simulation's transition to the turbulent state.

[1] Even though the defined Reynolds number in Eqn. (1) is inspired by the well-established one in fluid mechanics, we use a set of characteristics that describe or compromise the behavior of the crowd instead of using the classical properties of a fluid.

B. Force-based model

To simulate the behavior of the crowd, we use the Social Force Model. A common force-based model was introduced by Helbing and Molnar [19]. In this work, we follow the reinterpreted models presented in references [10, 11] since the original model does not account for physical forces, such as collisions.

The total force acting on each individual is given by

$$\mathbf{F}_i = \sum_{j\neq i}^{N}[\mathbf{f}_{ij}^I + \mathbf{f}_{ij}^C] + \sum_{w}^{M}[\mathbf{f}_{iw}^O + \mathbf{f}_{iw}^E] + \mathbf{f}_i^D, \tag{3}$$

where $\mathbf{F}_i$ is the total force acting on the i^{th} individual, j is the index of all other individuals in the environment, N denotes the total number of individuals, w denotes the index of an obstacle, M denotes the total number of obstacles in the environment and $\mathbf{f}_{ij}^I$, $\mathbf{f}_{ij}^C$, $\mathbf{f}_{iw}^O$, $\mathbf{f}_{iw}^E$, $\mathbf{f}_i^O$ are the interaction forces, collision force, obstacle force, environment force, and desired force, respectively.

The desired force drives people to the destination they want, for example, to the exit. It is defined as

$$\mathbf{f}_i^D = m_i\frac{\mathbf{v}_d - \mathbf{v}_i}{\tau_i}. \tag{4}$$

Here, m_i is the mass of the i^{th} individual, which is considered the same for all individuals. $\mathbf{v}_d$ is the desired velocity pointing from the individual towards the desired destination, while $\mathbf{v}_i$ is the actual velocity at time step t. τ_i is the time parameter which determines how quickly an individual accelerates to their desired velocity. When the velocity of an individual decreases, the desired force acting on it increases. A graphic representation is shown in FIG.1a.

The interaction force will drive one individual to move and keep a proper distance from the other. It is formulated as

$$\mathbf{f}_{ij}^I = A_i e^{\frac{r_{ij}-d_{ij}}{B_i}}\mathbf{n}_{ij}, \tag{5}$$

where A_i and B_i are positive constants, which determine the strength and effective range between the i^{th} and j^{th} individuals. r_{ij} is summed radii of the two individuals, while d_{ij} is the distance between them. The $\mathbf{n}_{ij}$ is the normalized vector that points from the i^{th} to the j^{th} individual. The interaction force characterizes an individual's willingness to maintain a distance to the others, as illustrated in FIG. 1b.

If a collision occurs, another force starts to act on the individual. This collision force is defined as,

$$\mathbf{f}_{ij}^C = \sigma(r_{ij} - d_{ij})(k_1\mathbf{n}_{ij} + k_2\Delta v_{ji}\mathbf{t}_{ij}). \tag{6}$$

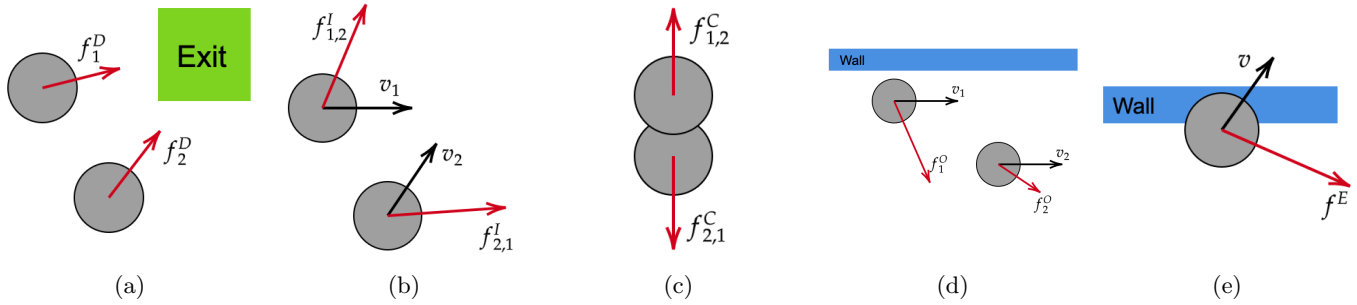

(a) (b) (c) (d) (e)

FIG. 1: Schematic representation of the (a) desired, (b) interaction, (c) collision, (d) obstacle and (e) environment forces presented, respectively, in Eqns. (4), (5), (6), (7), and (8) from §II B. The desired force (a) drives the individuals to the exit. The interaction force (b) and obstacle force (d) steers an individual away from another individual and wall respectively, based on the current position and velocity. Collision force (c) and environment force (e) occur on collision, and repel the individual from the collider.

r_{ij}, d_{ij}, and $\mathbf{n}_{ij}$ are the same quantities as explained in Eqn. (5), k_1 and k_2 are large constants that determine the effects of obstruction in the case of physical interactions. Δv_{ji} is defined as $(\mathbf{v}_i - \mathbf{v}_j)\cdot\mathbf{t}_{ij}$, where $\mathbf{t}_{ij}$ is the unit vector pointing in the tangential direction of the displacement between the two individuals. The sigma function implies that the collision force applies only if two individuals have contact. FIG. 1c shows a graphic representation of this force.

The collision and interaction forces occur in interactions between two individuals. For interaction with static obstacles, for instance walls, there are two analogous forces: the obstacle force and the environment force. The obstacle force drives an individual to move away from the obstacle in their path while the environment force occurs upon collision with the walls or other obstacles. The equations are given by

$$\mathbf{f}_{iw}^O = A_i e^{\frac{r_i - d_{iw}}{B_i}} \mathbf{n}_{iw}, \tag{7}$$

and

$$\mathbf{f}_{iw}^E = \sigma(r_i - d_{iw})(k_1 \mathbf{n}_{iw} - k_2(v_i \cdot \mathbf{t}_{iw})\mathbf{t}_{iw}), \tag{8}$$

where r_i denotes the radius of the i^{th} individual, d_{iw} is their distance to the w^{th} wall, with n_{iw} and t_{iw} being the normalized vectors defined in the previous equations. The above two forces are demonstrated by FIGS. 1d and 1e respectively.

C. Implementation

To simulate the dynamics of the social force model, a simple example case is constructed, where a crowd of individuals is trying to reach an exit at the end of a corridor. The setup can be seen in FIG. 2, where an arbitrary frame of a simulation is displayed.

Throughout the simulation, each individual generates a desired force towards the exit, as well as a social force in order to avoid collisions. If the area of this individual overlaps with another individual or a wall, an environmental force is applied in proportion to the velocity. The sum of magnitudes of these environmental forces acting on an individual defines the internal pressure. If the pressure exceeds a predefined threshold, the individual becomes a casualty and no longer interacts with others. Likewise, individuals that fully overlap with the exit area are considered out and, therefore, cease to be included in the force model calculations.

The simulation is implemented as a series of frames, as seen in FIG. 3, with each frame consisting of the complete state of each individual at the given time instance. Given an initial configuration, each frame is computed by applying Euler's method to the previous frame for a specified time step Δt [20]. Thus, the dynamics of the simulation is given by the system of equations,

$$\begin{cases} \mathbf{X}_i = \mathbf{X}_{i-1} + \mathbf{V}_i \Delta t \\ \mathbf{V}_i = \mathbf{V}_{i-1} + \mathbf{A}_i \Delta t \\ \mathbf{A}_i = \frac{\mathbf{F}_i}{m_i} \end{cases}, \tag{9}$$

where $\mathbf{F}_i$ is the total force defined in Eqn. (3).

Since each simulation is determined by the chosen constants of the system, they can be seen as parameters for the results. Thus, a simulation can be viewed as a function which maps a set of parameters to a simulation history, illustrated in FIG. 3. This history is then analyzed to extract metrics from the simulation. By running the simulation multiple times with a range of values for a parameter, one can determine the correlation between a parameter and the resulting metrics. In our case, the parameters of interest are the height of the room, H, the number of individuals, N, and desired speed, v_d, since these are the key variables that influence the Reynolds number. By varying these parameters, we obtain a set of simulation histories, which are then analyzed in order to obtain the relevant metrics.

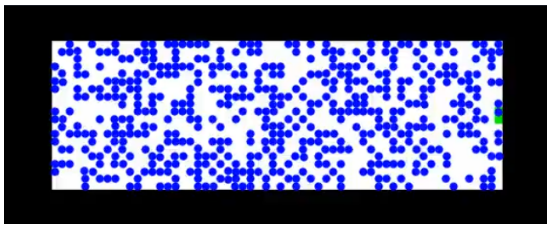

(a) Initial frame of a simulation.

(b) A frame where casualties have occurred.

FIG. 2: The evolution of a simulation from the initial state (a) to a late state (b). Each individual (blue circle) moves toward the exit (green area), while also trying to avoid collisions with each other and the wall (black border). When the pressure on an individual exceeds a threshold, they become a casualty (red circle). Parameters used for this simulation were:
$H = 20$ m (distance from bottom to top of room),
$N = 500$ (number of individuals),
$v_d = 10$ m/s (desired velocity of each individual).

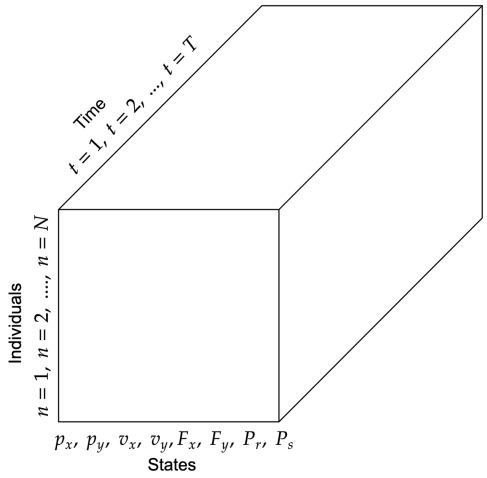

FIG. 3: Representation of a simulation history. Each frame is represented by a state for a given individual. The state consists of the position $\mathbf{p}$, the velocity $\mathbf{v}$, the net force $\mathbf{F}$, the pressure P_r, and the status P_s.

III. RESULTS

We identify four important variables to characterize the state of the crowd during the simulation: the fraction of individuals who exit the room and the fraction of casualties, as explained in §II C, the alignment coefficient Ψ_c as introduced in §II, and the averaged individual density $\bar{\rho}_{\mathrm{I}}$ defined by computing the density within a unit circle around each individual and then taking the average over the entire population. Readers should not confuse $\bar{\rho}_{\mathrm{I}}$ with the density parameter used for the pseudo-Reynolds number in §II Eqn. (1).

The fraction of individuals in the two states allow us to analyze the exiting rate and the likelihood of casualties. The alignment coefficient, Ψ_c, and the averaged individual density, $\bar{\rho}_{\mathrm{I}}$, are used to analyze whether the crowd flow is laminar or turbulent and whether the crowd is clustering.

FIG. 4 shows the evolution of the four variables over time under different pseudo-Reynolds numbers Re_c. FIG. 4a plots the averaged individual density $\bar{\rho}_{\mathrm{I}}$ versus time. The crowd is significantly more clustered at high pseudo-Reynolds numbers, $\mathrm{Re}_c = 250$ and 500. This is due to at higher Re_c's, the chance of casualties is greatly increase (cf. FIG. 4c), and the remaining individuals are allowed to overlap with individuals that are turned into casualties to simulate the 'stampedes' effects in crowd disasters, as explained in §II C. This effect also resembles the compressibility of fluids [12].

FIG. 4b shows the alignment coefficient Ψ_c of the crowds in various simulation settings. We can see that they all follow a similar pattern for different Re_c's. The coefficients peak quickly at around $\Psi_c = 0.6 \sim 0.8$ when the crowd starts to move towards the exit, then the coefficients decay when the crowd clusters around the exit.The evolution of the alignment coefficients demonstrates the transition from laminar to turbulent state of the crowd. At lower pseudo-Reynolds numbers, that is, $\mathrm{Re}_c = 46.9$ and 100, the coefficients peak higher ~ 0.8 and decay slower. This indicates that the lower Re_c's maintain the laminar states longer, as predicted by the fluid theories. The red dashed-dotted line maintains the highest alignment coefficient at the end of the simulation despite having the largest pseudo-Reynolds number $\mathrm{Re}_c = 500$. This is because it has the lowest room height $H = 10$ m, from which we see that the geometry design of the room also has impacts on the crowd dynamics.

FIGs. 4c and 4d show the fraction of individuals who exit the room and the fraction of casualties, respectively. From FIG. 4c, we see that there is no casualty at low pseudo-Reynolds numbers, $\mathrm{Re}_c = 46.9$ and 100. A surprising finding is that the simulation with $\mathrm{Re}_c = 500$ has a casualty rate similar to $\mathrm{Re}_c = 250$ in the middle section of the simulation. This may also be due to the narrower room design, $H = 10$ m vs. $H = 20$ m, as emphasized in the previous paragraph. In FIG. 4d, none of the exiting rates is ideal; this may be due to the small exit size implemented in the simulations. The orange dashed line

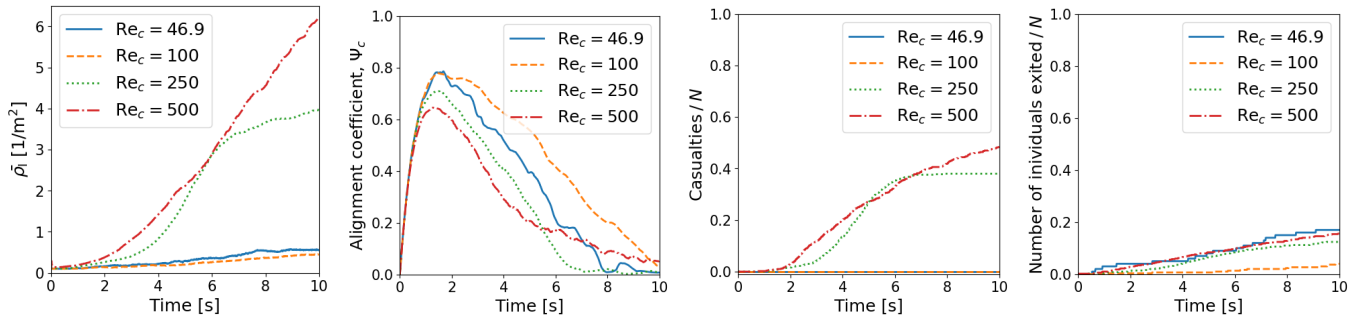

FIG. 4: (a) Averaged individual density, $\bar{\rho}_{\mathrm{I}}$. (b) Alignment coefficient, Ψ_c. (c) Fraction of casualties among the crowd. (d) Fraction of exited individuals among the crowd.
Solid blue line: $\mathrm{Re}_c = 46.9$ ($N = 100, H = 15$ m, $v_{\mathrm{d}} = 7.5$ m/s),
Dashed orange line: $\mathrm{Re}_c = 100$ ($N = 300, H = 15$ m, $v_{\mathrm{d}} = 5$ m/s),
Dotted green line: $\mathrm{Re}_c = 250$ ($N = 500, H = 20$ m, $v_{\mathrm{d}} = 10$ m/s),
Dashed-dotted red line: $\mathrm{Re}_c = 500$ ($N = 500, H = 10$ m, $v_{\mathrm{d}} = 10$ m/s).

with the lowest desired speed $v_{\mathrm{d}} = 5$ m/s has the worst exiting rate. Simulations with a higher desired speed, i.e. the dotted green line and dashed-dotted red line, have $v_{\mathrm{d}} = 10$ m/s, have slightly higher exiting rate, even though they have higher pseudo-Reynolds numbers.

The fraction of casualties is the critical variable to characterize crowd disasters. From the figures above, we find that $\mathrm{Re}_c \gtrsim 250$ results in casualties. To better understand which parameters have the most critical impacts on crowd safety, we performed multiple simulations with various parameter settings and compared the resulting fractions of casualties in the end, as shown in FIG. 5. In FIG. 5a, we fixed the room height $H = 10$ m and plotted the casualty rates against population sizes N at three different desired speeds v_{d}. Even in cases with high desired speed $v_{\mathrm{d}} = 10$ m/s, there were no casualties when the population size is small, $N = 100$. The chance of casualties increased significantly with population size N. FIG. 5b shows the casualty rates against the desired speed v_{d}, which revealed similar tendencies to those of FIG. 5a.

In FIG. 5c, we fixed the population size $N = 500$ and investigated the impact of room height. Although we see that the chance of casualties decreases as the room height increases, the slopes are flatter than in the previous two plots. Combining the results from previous paragraphs, which show that narrower rooms can lead to higher exit rates and alignment coefficients, we conclude that a lower room height H may help prevent crowd disasters.

IV. CONCLUSIONS

In this report, we studied the complex behaviors that emerge from the dynamics of human crowds and investigated the potential causes of crowd disasters. The problem was approached both analytically and numerically. We combined a social force-based model with physical contact forces to numerically simulate human crowds. This hybrid model was then used to simulate the emergency situation of a crowd leaving a room. From the analytical aspect, we treated the crowds as fluids. Inspired by fluid mechanics, we defined a pseudo-Reynolds number Re_c to characterize the general properties of the crowd and the geometry of the room. Furthermore, we introduced an alignment coefficient Ψ_c to understand the collective dynamics of simulated individuals. The above two parameters allow us to investigate whether the crowd is in a laminar (individuals moving in an ordered manner) or turbulent (individuals clustering and unable to exit the room) state.

We ran multiple simulations with different pseudo-Reynolds numbers and concluded that $\mathrm{Re}_c \gtrsim 250$ would lead to casualties. We also found that the probability of casualties is strongly correlated with the population size N and the desired speed v_{d} which measures the crowd's stress level. Another interesting finding was that a narrower room design can have some positive impacts on crowd dynamics. Due to time limitations and lack of computational resources, we were unable to run simulations on larger scales or perform more comprehensive analysis to identify other crowd fluid features. However, features such as waves, boundary layers, and vortices can be visualized from our animations in the supplement materials which can be found on our GitHub repository [21].

Many potential improvements and further work can be added to our project. We would like to compare our simulations with real-life data [22] to validate our numerical model and analysis. As reported by news, real crowd disasters usually involve populations exceeding 10,000 individuals [3]. Thus, we would like to run larger scale simulations on super computers. With a larger number of individuals, more fluid features may emerge from the simulations. Following our findings in §III, the geometry

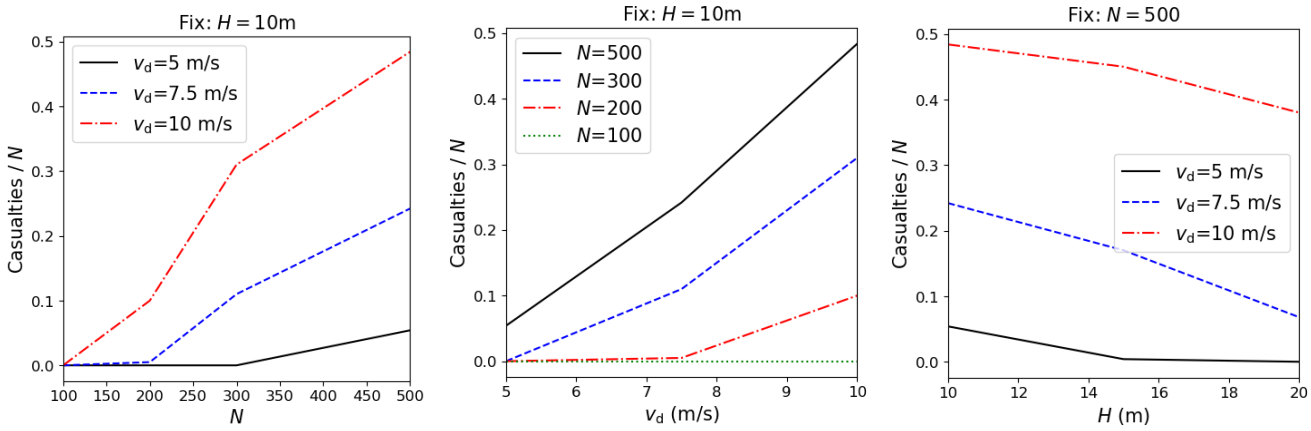

(a) (b) (c)

FIG. 5: (a) Fractions of casualties versus Number of individuals, N. Fix height of the room, $H = 10$ m. (b) Fractions of casualties versus Desired speed, v_d. Fix height of the room, $H = 10$ m. (c) Fractions of casualties versus height of the room, H. Fix number of individuals, $N = 500$. Dependency of casualties on the three parameters: Number of individuals N, Desired speed v_d, Height of the room H.

design of the room impacts crowd dynamics, and further investigations can be made. Overall, even though there is existing research, this problem is a complex topic. Therefore, new research has room for improvement, giving crowd disasters good prospects as an active research field.

CONTRIBUTIONS

A.G. Implementation (Primary), Social force model (Secondary), Result analysis (Secondary).

M.L. Fluid model (Primary), Result analysis (Secondary).

N.U. Literature review (Primary), Implementation (Secondary).

R.Q. Social force model (Primary), Implementation (Secondary).

R.Z. Fluid model (Primary), Result analysis (Primary).

All authors contributed equally to the presentation and report.

ACKNOWLEDGMENTS

The authors would like to thank Dr. Agnese Callegar and Team Lizards for the fruitful talks and constructive suggestions on the project.

[1] Nicolas Bain and Denis Bartolo. Dynamic response and hydrodynamics of polarized crowds. *Science*, 363(6422): 46–49, 2019. doi:10.1126/science.aat9891.

[2] Wikipedia. Crowd collapses and crushes, 2022. URL `https://en.wikipedia.org/wiki/Crowd_collapses_and_crushes`. Accessed: 2022-11-20.

[3] Wikipedia. List of fatal crowd crushes, 2022. URL `https://en.wikipedia.org/wiki/List_of_fatal_crowd_crushes`. Accessed: 2022-12-16.

[4] Maria Pretorius, Steven Gwynne, and Edwin R Galea. Large crowd modelling: an analysis of the duisburg love parade disaster. *Fire and Materials*, 39(4):301–322, 2015.

[5] Amy Tikkanen. Hillsborough disaster, 2022. URL `https://www.britannica.com/event/Hillsborough-disaster`. Accessed: 2023-01-03.

[6] Working With Crowds. Hajj pilgrimage: More than 2000 dead in crush near mecca. URL `https://www.workingwithcrowds.com/hajj-pilgrimage-2000-dead-crush-near-mecca/`. Accessed: 2023-01-02.

[7] Kim Han-joo. Death toll from halloween crowd crush rises to 158, 2022. URL `https://en.yna.co.kr/view/AEN20221114000700315`. Accessed: 2023-01-03.

[8] Libo Sun and Norman I Badler. Exploring the consequences of crowd compression through physics-based simulation. *Sensors*, 18(12):4149, 2018.

[9] Shanwen Yang, Tianrui Li, Xun Gong, Bo Peng, and Jie Hu. A review on crowd simulation and modeling. *Graphical Models*, 111:101081, 2020. ISSN 1524-0703. doi:https://doi.org/10.1016/j.gmod.2020.101081. URL `https://www.sciencedirect.com/science/article/pii/S1524070320300242`.

[10] Dirk Helbing, Illés Farkas, and Tamás Vicsek. Simulating dynamic features of escape panic. *Nature*, 407:487–490,

09 2000. doi:10.1038/35035023.

[11] Peng Wang. *Understanding Social-Force Model in Psychological Principles of Collective Behavior*. PhD thesis, 10 2017.

[12] Roger L. Hughes. The flow of human crowds. *Annual Review of Fluid Mechanics*, 35(1):169–182, 2003. doi: 10.1146/annurev.fluid.35.101101.161136.

[13] On the fluid mechanics of human crowd motion. *Transportation Research*, 8(6):509–515, 1974. ISSN 0041-1647. doi:https://doi.org/10.1016/0041-1647(74)90027-6.

[14] Michael Eckert. *The Dawn of Fluid Dynamics: A Discipline Between Science and Technology*. John Wiley & Sons, 2007.

[15] G. K. Batchelor. *Flow at Large Reynolds Number: Effects of Viscosity*, page 264–377. Cambridge Mathematical Library. Cambridge University Press, 2000. doi: 10.1017/CBO9780511800955.007.

[16] Gregory Falkovich. *Fluid Mechanics*. Cambridge University Press, 2 edition, 2018. doi:10.1017/9781316416600.

[17] L.D. Landau and E.M. Lifshitz. *Fluid Mechanics*. A-W series in advanced physics. ISBN 9780080091044.

[18] Arnold Sommerfeld. Ein beitrag zur hydrodynamischen erkläerung der turbulenten flüssigkeitsbewegüngen (a contribution to hydrodynamic explanation of turbulent fluid motions). International Congress of Mathematicians, 1908.

[19] Dirk Helbing and Péter Molnár. Social force model for pedestrian dynamics. *Phys. Rev. E*, 51:4282–4286, May 1995. doi:10.1103/PhysRevE.51.4282.

[20] David F. Griffiths and Desmond J. Higham. *Euler's Method*, pages 19–31. Springer London, London, 2010.

[21] Gasparyan Artur, Maria Li López Bautista, Nina Uljanic, Rundong Zhou, and Ruiqi Qiu. Crowd Disasters Simulation (CDS). URL `https://github.com/gasparyanartur/crowd-disasters`.

[22] Sébastien Motsch, Mehdi Moussaid, Elsa G. Guillot, Mathieu Moreau, Julien Pettré, Guy Theraulaz, Cecile Appert-Rolland, and Pierre Degond. Modeling crowd dynamics through coarse-grained data analysis. *Mathematical Biosciences and Engineering*, 15(6):1271–1290, 2018. doi:10.3934/mbe.2018059.